universe

IMPACT FACTOR 2.813

CITESCORE 3.2

Article

Reconstructing Torsion Cosmology from Interacting Holographic Dark Energy Model

Song Li and Yun Chen

Special Issue

Quantum Entanglement and Holographic Universe

Edited by

Dr. Rong-Xin Miao

MDPI

https://doi.org/10.3390/universe9020100

universe

MDPI

Article

Reconstructing Torsion Cosmology from Interacting Holographic Dark Energy Model

Song Li [1,*] and Yun Chen [2,3]

[1] Department of Physics, Capital Normal University, Beijing 100048, China
[2] Key Laboratory for Computational Astrophysics, National Astronomical Observatories, Chinese Academy of Sciences, Beijing 100012, China
[3] College of Astronomy and Space Sciences, University of Chinese Academy of Sciences, Beijing 100049, China
* Correspondence: sli@cnu.edu.cn

Abstract: We consider a cosmological model in the framework of Einstein–Cartan theory with a single scalar torsion $\phi = \phi(t)$ and reconstruct the torsion model corresponding to the holographic dark energy (HDE) density. By studying the corresponding relation between the effective energy density of torsion field ρ_ϕ and holographic dark energy density ρ_{HDE}, we naturally obtain a kind of torsion field from the interacting holographic dark energy with interaction term $Q = -2\phi\rho_m$ and ρ_m is the energy density of matter. We analyze the reconstructed torsion model and find that the torsion field behaves like the quintessence $(w > -1)$ or quintom (exhibiting a transition from $w > -1$ to $w < -1$) dark energy, depending on the value of the model parameter c. We then perform a stability analysis according to the squared sound speed. It is shown that the model is classically stable in the current epoch for the case of $c < 1$. We also investigate the model from the viewpoint of statefinder parameters and it turns out that the statefinder trajectories in the $r - s$ plane behave differently for the three cases of c and also quite distinct from those of other cosmological models. From the trajectories of the statefinder pair $\{q, r\}$, we find that, for all the three cases of c, the universe has a phase transition from deceleration to acceleration, consistently with cosmological observations. In addition, we fit the reconstructed torsion model with the recent Type Ia supernovae (SNe Ia) samples, i.e., the Pantheon sample containing 1048 SNe Ia with the redshift in the range $0.01 < z < 2.3$ and the Pantheon+ sample with 1701 light curves of 1550 distinct SNe Ia in the range $0.001 < z < 2.26$. The analysis results show that the limits on the present fractional energy density of matter Ω_{m0} are completely compatible with those of the ΛCDM model obtained from the latest Planck mission observations at 68% confidence level. The mean value of c constrained from the Pantheon sample corresponds to the quintom-like scenario (i.e., $c < 1$) and its mean value from the Pantheon+ sample corresponds to the quintessence-like scenario (i.e., $c \geq 1$). However, both of the Pantheon and Pantheon+ samples cannot distinguish the quintom-like and quintessence-like scenarios at 68% confidence level.

Keywords: torsion field; holographic dark energy; universe

Citation: Li, S.; Chen, Y. Reconstructing Torsion Cosmology from Interacting Holographic Dark Energy Model. *Universe* **2023**, *9*, 100. https://doi.org/10.3390/universe9020100

Academic Editor: Rong-Xin Miao

Received: 22 January 2023
Revised: 11 February 2023
Accepted: 13 February 2023
Published: 16 February 2023

1. Introduction

Current observations suggest that our universe is undergoing a period of accelerated expansion [1,2]. Within the framework of general relativity (GR), the cosmic speed-up is attributed to the contribution of a spatially homogeneous and gravitationally repulsive energy component (roughly 70 percent), called dark energy. The flat ΛCDM model, with the constant equation of state, seems to be the simplest explanation for the phenomenon and predicts quite well during the overall evolution of the universe. Furthermore, recent analysis indicates that there exist some specific observational discrepancies at both small scales and large scales [3–6]. Moreover, in recent decades, the dynamical scenarios of dark energy have been widely tried out. Nevertheless, none of these attempts stemming from comparatively poor theoretical motivation turn out to be problem-free and the nature of dark energy still remains a mystery.

In view of the challenge and the fact that gravity is the only dominant long-range interaction insofar as we know, it is reasonable to consider the possibility that we have not fully understood the character of gravity on a cosmological scale. Therefore, the exploration of alternative theories of gravity are proposed and the explanation of the accelerated expansion of the universe from fundamental physics is now a great challenge. These categories are known as modified gravity theories, based on the introduction of either geometric terms or extra degrees of freedom in the Einstein–Hilbert action [7–9].

As a natural extension of Einstein's theory of general relativity, the Einstein–Cartan (EC) theory of gravity [10–14] based on a new connection which allows the former to have a symmetric (the standard Christoffel part) and a new anti-symmetric part called contortion, is purely geometrical modifying of the Einstein equations, unlike extensions which invoke new fields from the metric. It is a physically consistent theory, unlike some theories with non-symmetric metric which do have deficiencies. The EC theory takes into account the spin properties of matter and describes their influence on the geometrical structure of spacetime called Riemann–Cartan spacetime, which is characterized by non-trivial curvature and torsion. However, background torsion breaks the weak equivalence principle [15,16] and violates local Lorentz invariance [17]. Moreover, there is no experimental or observational evidence to support the distinctive predictions of the EC theory or the existence of torsion. The main reason is that the theory only deviates from classical general relativity at extremely high energy densities. Nevertheless, the EC theory has been neither confirmed nor denied so far. Its appeal lies in the cosmological aspects. The EC theory could provide some answers to the unresolved questions of modern theoretical physics and astrophysics, such as dark energy effects, the recently discovered universal acceleration [18–20], inflationary models [21,22], torsion as an alternative to dark matter [23,24] and so on.

In this paper, we study the torsion effects in a Friedmann cosmology as a candidate to dark energy in the universe. As mentioned in [25], the spatially homogeneous and isotropic Friedmann–Lemaître–Robertson–Walker (FLRW) universe can only accommodate specific forms of torsion. In the work of [26], which focused on finding exact solutions for torsional Friedmann-like models, the torsion fields, determined by a single scalar function of time $\phi = \phi(t)$, are generally compatible with the FLRW symmetries. Here, we adopt the same named torsion field $\phi(t)$ as [26] and reconstruct a torsion model corresponding to the holographic dark energy (HDE) density. The HDE model is based on the holographic principle with Bekenstein–Hawking entropy and the Hubble horizon as its IR cutoff [27]. However, when the Hubble horizon is chosen as the IR cut-off, a non-accelerated expansion universe can be achieved. Its shortcomings in describing the history of a flat FLRW universe have motivated some tentative changes in this model. For instance, in the literature [28], the vacuum energy is viewed as dark energy and is related to the event horizon of the universe when we require that the zero-point energy of the system should not exceed the mass of a black hole with the same size. In this way, the HDE model can derive an accelerated expansion universe. Moreover, it has been constrained with different observational data and is consistent with the data [29,30]. In the reconstructed torsion model, we analyze the behavior of the torsion field, the matter density, the effective torsion equation of state parameter, as well as the classical stability of our model. Additionally, we apply the statefinder parameters to the model to reveal differential feature in contrast with other cosmological models. Finally, we prove that the reconstructed torsion model is consistent with recent observations and thus provides a good candidate for the description of an expansional universe.

The rest of the paper is organized as follows: In Section 2, we present the main equations of Friedmann cosmology with torsion, based on [26]. In Section 3, we reconstruct a torsion model from the interacting HDE and study the dynamical behavior of the torsion field in a spatially flat FLRW universe. In Section 4, constraints from the updated observational data are obtained for the torsion model. In the end, the conclusions are summarized in Section 5. Throughout the entire manuscript, we assume today's scale

factor $a_0 = 1$, so the redshift $z = a^{-1} - 1$; the subscript "0" always indicates the present value of the corresponding quantity and the unit with $c = \hbar = 1$ is used.

2. FLRW Cosmology with Torsion

The affine connection and the curvature tensor in the Riemann–Cartan spacetime are defined as

$$\Gamma^{\lambda}{}_{\mu\nu} = \tilde{\Gamma}^{\lambda}{}_{\mu\nu} + K^{\lambda}{}_{\mu\nu}, \tag{1}$$

$$\begin{aligned} R_{\mu\nu\sigma}{}^{\rho} = {} & \tilde{R}_{\mu\nu\sigma}{}^{\rho} - \partial_{\mu}K^{\rho}{}_{\nu\sigma} + \partial_{\nu}K^{\rho}{}_{\mu\sigma} + \tilde{\Gamma}^{\rho}{}_{\nu\lambda}K^{\lambda}{}_{\mu\sigma} \\ & + \tilde{\Gamma}^{\lambda}{}_{\mu\sigma}K^{\rho}{}_{\nu\lambda} + K^{\rho}{}_{\nu\lambda}K^{\lambda}{}_{\mu\sigma} - \tilde{\Gamma}^{\rho}{}_{\mu\lambda}K^{\lambda}{}_{\nu\sigma} \\ & - \tilde{\Gamma}^{\lambda}{}_{\nu\sigma}K^{\rho}{}_{\mu\lambda} - K^{\rho}{}_{\mu\lambda}K^{\lambda}{}_{\nu\sigma}, \end{aligned} \tag{2}$$

where $\tilde{\Gamma}^{\lambda}{}_{\mu\nu}$ is the Levi–Civita connection, $\tilde{R}_{\mu\nu\sigma}{}^{\rho}$ is the Riemann curvature tensor, $K^{\lambda}{}_{\mu\nu} = T^{\lambda}{}_{\mu\nu} + T_{\mu\nu}{}^{\lambda} + T_{\nu\mu}{}^{\lambda}$ is the contorsion and $T^{\lambda}{}_{\mu\nu} = \Gamma^{\lambda}{}_{[\mu\nu]}$ represents Cartan's torsion tensor.

Starting from the action of the Einstein–Cartan theory

$$S_{EC} = \int d^4x\sqrt{-g}\left(-\frac{R(\Gamma)}{2\kappa^2} + L_m\right), \tag{3}$$

where $\kappa^2 = 8\pi G$, g is the determinant of the spacetime metric tensor $g_{\mu\nu}$, R is the Ricci–Cartan curvature scalar and L_m represents the Lagrangian of matter fields, the field equations are given by

$$R_{\mu\nu} - \frac{1}{2}Rg_{\mu\nu} = \kappa^2\tau_{\mu\nu}, \tag{4}$$

with $R_{\mu\nu}$ and $\tau_{\mu\nu}$ representing the Ricci–Cartan tensor and the energy-momentum tensor of the matter, respectively, and

$$T_{\alpha\mu\nu} = -\frac{1}{4}\kappa^2\left(2\sigma_{\mu\nu\alpha} + g_{\nu\alpha}\sigma_{\mu} - g_{\alpha\mu}\sigma_{\nu}\right), \tag{5}$$

where $\sigma_{\mu\nu\alpha} = \sigma_{[\mu\nu]\alpha}$ and $\sigma_{\mu} = \sigma^{\alpha}{}_{\mu\alpha}$ are, respectively, the spin tensor and the spin vector of the matter. The first Einstein–Cartan equation maintaining the same form of standard general relativity relates the curvature of spacetime to the energy-momentum density of matter, but without having the symmetry of both the Ricci–Cartan and energy-momentum tensors (i.e., $R_{[\mu\nu]} \neq 0$ and $\tau_{[\mu\nu]} \neq 0$) due to the presence of torsion. Equation (4) exhibits extra contributions to both energy density and pressure of matter, through the products of the spin density [31]. The energy-momentum density of matter is typically coupled to the spin of the matter via the second Cartan field Equation (5) [12]. The common assumption is that the spacetime torsion is induced by the spin of the matter, just like the curvature is generated by the matter's energy-density contribution.

Following [26], in a homogeneous and isotropic Friedmann background, the torsion tensor takes the form

$$T_{\alpha\mu\nu} = 2\phi h_{\alpha[\mu}u_{\nu]}, \tag{6}$$

and then the associated torsion vector is given by

$$T_{\alpha} = T^{\mu}{}_{\alpha\mu} = -3\phi u_{\alpha}, \tag{7}$$

where $\phi = \phi(t)$ is a scalar function that depends only on time, u_{α} is a timelike four-velocity vector (i.e., $u_{\alpha}u^{\alpha} = -1$) and the projection tensor $h_{\mu\nu} = g_{\mu\nu} + u_{\mu}u_{\nu}$ is a symmetric spacelike tensor orthogonal to u_{μ} (i.e., $h_{\mu\nu} = h_{\nu\mu}, h_{\mu\nu}u^{\nu} = 0, h_{\mu}{}^{\mu} = 3$). Considering the Cartan field Equation (5), one can recast relations (6) and (7) into the expressions $\kappa^2\sigma_{\alpha\mu\nu} = 8\phi h_{\nu[\alpha}u_{\mu]}$ and $\kappa^2\sigma_{\alpha} = 12\phi u_{\alpha}$ for the spin tensor and the spin vector, respectively [26]. Combining with relations (6) and (7), the above expressions in turn lead to the relations $T_{\alpha\mu\nu} = -\frac{1}{4}\kappa^2\sigma_{\nu\mu\alpha}$

and $T_\alpha = -\frac{1}{4}\kappa^2\sigma_\alpha$ between the torsion and the spin fields. Given that the two fields are simply proportional to each other and both fully determined by the scalar function ϕ, we will focus on torsion rather than spin in the following.

Considering a spatially flat Friedmann–Lemaître–Robertson–Walker (FLRW) universe with the metric:

$$ds^2 = -dt^2 + a^2(t)[dr^2 + r^2(d\theta^2 + \sin^2\theta d\varphi^2)], \tag{8}$$

where t is the cosmic time, $a(t)$ is the scale factor and r, θ, φ are the comoving coordinates, relation (6) leads to the non-zero components of the torsion tensor: $T^i{}_{0i} = -T^i{}_{i0} = \phi$ (with $i = 1, 2, 3$). Together with (1) and (2), the Ricci scalar of an FLRW-like spacetime with non-zero torsion reads (see [26] for details):

$$R = 6\Big(\dot{H} + 2H^2 + 2\dot{\phi} + 6H\phi + 4\phi^2\Big), \tag{9}$$

where $H = \dot{a}/a$ is the Hubble parameter. Then, from Equation (4), by introducing the energy-momentum tensor of a perfect fluid, the Friedmann equations including a general matter density ρ_m and pressure of matter p_m are written in the equivalent forms of those in general relativity as

$$H^2 = \frac{\kappa^2}{3}(\rho_m + \rho_\phi), \tag{10}$$

$$2\dot{H} + 3H^2 = -\kappa^2(p_m + p_\phi), \tag{11}$$

where ρ_ϕ and p_ϕ satisfying

$$\rho_\phi = -\frac{12}{\kappa^2}(\phi + H)\phi \tag{12}$$

and

$$p_\phi = \frac{4}{\kappa^2}(\dot{\phi} + 2H\phi + \phi^2) \tag{13}$$

stand for the torsion contribution to the energy density and pressure, respectively. Therefore, the corresponding effective torsion equation of state (EoS) is given by

$$w_\phi \equiv \frac{p_\phi}{\rho_\phi} = -1 + \frac{2\phi^2 + H\phi - \dot{\phi}}{3\phi(H + \phi)}. \tag{14}$$

We can remark that $\dot{\phi}/H^2 > 2(\phi/H)^2 + \phi/H$ exhibits a phantom-like dark energy ($w_\phi < -1$) and $\dot{\phi}/H^2 < 2(\phi/H)^2 + \phi/H$ is for a quintessence-like one ($w_\phi > -1$) when $\phi/H > 0$ or $\phi/H < -1$ and vice versa for the case of $-1 < \phi/H < 0$.

Following Equation (10), the torsional analogue of the Friedmann equation recasts as

$$\Omega_m + \Omega_\phi = 1, \tag{15}$$

where $\Omega_m = \rho_m/\rho_{cr}$ and $\Omega_\phi = \rho_\phi/\rho_{cr}$, with $\rho_{cr} = 3H^2/\kappa^2$ representing the critical density of the universe. The dimensionless parameter $\Omega_\phi = -4[1 + (\phi/H)](\phi/H)$ monitors the torsion contribution to the total energy density of the universe and the dimensionless variable ϕ/H measures the contribution of the torsion field relative to that of the Hubble expansion. We note that the torsion contribution Ω_ϕ can be either positive or negative, depending on the sign of ϕ/H. It can be easily seen that $\Omega_\phi = 0$ when $\phi/H = 0, -1$ and torsion dominates completely when $\phi/H = -1/2$, which translates into $\Omega_\phi = 1$.

For barotropic matter satisfying an EoS of the form $p_m = w\rho_m$, the continuity equation reads:

$$\dot{\rho}_m + 3(1 + w)H\rho_m + 2(1 + 3w)\phi\rho_m = 0, \tag{16}$$

which can be integrated to

$$\rho_m(z) = \rho_{m0}(1+z)^{3(1+w)} \exp\left[2(1+3w)\int_0^z \left(\frac{\phi}{H}\right)\frac{dz}{1+z}\right], \tag{17}$$

when $w =$ constant. Accordingly, we can depict the effect of torsion on the energy-density evolution via the exponential term on the right-hand side of the above. Obviously, it depends on the EoS of the matter. The torsion contribution to the energy density vanishes in the special case of a medium with $w = -1/3$. On the other hand, the energy-density evolution becomes essentially torsion dominated in the case of a vacuum stress with $w = -1$.

Substituting Equation (16) into Equatins (10) and (11), we obtain

$$\dot{\rho}_m + 3(1+w)H\rho_m = Q, \tag{18}$$

$$\dot{\rho}_\phi + 3(1+w_\phi)H\rho_\phi = -Q, \tag{19}$$

with the interaction term $Q = -2(1+3w)\phi\rho_m$ representing the energy exchange between the torsion field and matter. Q should be positive as the energy is transferred to the usual fluid and vice versa for a negative Q. Therefore, the non-zero interaction generally exists due to the presence of torsion and the effect of interaction on the energy-density evolution is characterized in Equation (17). Combining Equations (18) and (19), we obtain a derivative equation of $\dot{H}$ and $\dot{\Omega}_\phi$

$$2(\Omega_\phi - 1)\frac{\dot{H}}{H} + \dot{\Omega}_\phi + 3H(1+w)(\Omega_\phi - 1) = -H\Omega_I, \tag{20}$$

where the effective dimensionless quantity $\Omega_I \equiv Q/(H\rho_{cr}) = -2(1+3w)(1-\Omega_\phi)\phi/H$ is defined for interaction.

Integrating (16) and then the Friedmann Equation (10) can be recast into

$$E^2(z) = \frac{1-\Omega_{\phi 0}}{1-\Omega_\phi}\exp\left[3\int_0^z (1+w+\frac{2}{3}\frac{\phi}{H})\frac{dz}{1+z}\right], \tag{21}$$

where $E(z) = H(z)/H_0$ is the dimensionless Hubble parameter.

In order to better understand the influence of torsion field to the recent accelerated phase of expansion of the universe, we pay attention to the deceleration parameter $q = -\ddot{a}a/\dot{a}^2$, which can be written as

$$q = \frac{1}{2}(1+3w)(1-\Omega_\phi) + 2\frac{\dot{\phi}}{H^2} + 2\frac{\phi}{H}. \tag{22}$$

We notice that the torsion field can either assist or inhibit accelerated expansion ($q < 0$). For instance, the presence of torsion tends to accelerate the expansion when ϕ is constant and negative [26].

3. Torsion Reconstruction from Interacting HDE Model

In view of the absence of experimental or observational evidence to support the distinctive predictions of the existence of torsion and the EC theory as an alternative theory of mystery candidate, it is necessary to investigate how this theory can describe the HDE model, even though the holography principle is conjectured in the framework of the semi-classical Einstein gravity without torsion and is independent of details of the quantum state of matter, such as its spin. In the literature [32], the reconstruction scheme via HDE model in the modified theory of gravity with torsion is developed and it is found that the reconstructed model may cross the phantom line in the future. The reconstructed torsion models from the entropy-corrected holographic and new agegraphic dark energy can

also be found in [33,34]. In this paper, we make an attempt to consider a correspondence between torsion field and the holographic dark energy (HDE) [28] with the density given by

$$\rho_{HDE} = \frac{3c^2}{\kappa^2 {R_h}^2}, \tag{23}$$

where c is a dimensionless model parameter, which can only be determined by observation. It should be noted that a positive constant c is favored by the latest observational data [29,30]. The future event horizon of the universe, R_h, is defined as

$$R_h = a\int_t^\infty \frac{dt}{a} = a\int_a^\infty \frac{da}{Ha^2}. \tag{24}$$

The HDE model has been proved to be a competitive and promising dark energy candidate. Combining (23) and (24), we obtain

$$\frac{\dot{\Omega}_{HDE}}{2\Omega_{HDE}} + H + \frac{\dot{H}}{H} = H\sqrt{\frac{\Omega_{HDE}}{c^2}}, \tag{25}$$

where $\Omega_{HDE} = \rho_{HDE}/\rho_{cr}$ is the fractional energy density of HDE. Replacing Equation (23) in relation (12), i.e., $\rho_\phi = \rho_{HDE}$, yields the following equation

$$\left(\frac{\phi}{H}\right)^2 + \frac{\phi}{H} + \frac{1}{4}\Omega_{HDE} = 0. \tag{26}$$

Solving the equation, we obtain $\phi/H = \left(-1 \pm \sqrt{1-\Omega_{HDE}}\right)/2$. For a dust-like matter ($w = 0$), the deceleration parameter $q > 0$ when $\Omega_{HDE} \to 0$ (i.e., $z \to \infty$) is satisfied by a solution of the form

$$\frac{\phi}{H} = \frac{1}{2}(-1 + \sqrt{1-\Omega_{HDE}}), \tag{27}$$

which is the torsion field corresponding to the interacting HDE model. Clearly, the sign of ϕ/H is negative and its value is in the interval $-1/2 < \phi/H < 0$.

Combining (20) and (25), we obtain the following differential equation

$$\frac{d\Omega_{HDE}}{dz} = -\frac{2\Omega_{HDE}(1-\Omega_{HDE})}{1+z}\left[\sqrt{\frac{\Omega_{HDE}}{c^2}} + \frac{1}{2} - \frac{\Omega_I}{2(1-\Omega_{HDE})}\right], \tag{28}$$

which can be solved numerically and will be used in the data analysis procedure.

Taking into account the expression (27), we can numerically extract the evolution of the dimensionless ratio ϕ/H versus redshift. In order to compare with the current observational data, we consider the cases of $c = 0.8$, 1 and 1.2, as examples respectively, and adopt $\Omega_{m0} = 0.27$ in the detailed numerical analyses. The results are listed in Figure 1. It is evident that ϕ/H has a negative relationship with redshift. The ratio ϕ/H decreasing monotonically from zero at early times, i.e., at large z, to $-1/2$ in the far future (i.e., $z \to -1$), indicates an evolution towards a completely dark energy dominated epoch predicted via this model.

From Equation (17), the behavior of the dimensionless ratio ρ_m/ρ_{m0} in terms of redshift is shown in Figure 2. We observe that the energy density of matter is an increasing function of redshift z and remains positive as the universe expands for all the three values of c. Although the three cases of c deviate slightly at early times, they gradually decrease to zero at late time, as expected. This means that the universe exhibits the usual thermal history, with the successive sequence of matter and torsion epochs and with the transition to acceleration in agreement with the observational results. On the other hand, Figure 2 describes the effect of interaction Q on the energy density of matter. It is clear through the figure that the evolutionary trajectory of ρ_m/ρ_{m0} departs from the one of the non-interacting model, i.e., $\rho_m/\rho_{m0} = (1+z)^3$, at early times. The torsion model gradually closes to the

non-interacting model, converges to it at the present time (i.e., $z = 0$) and then slightly deviates from it at the late time, independent of c.

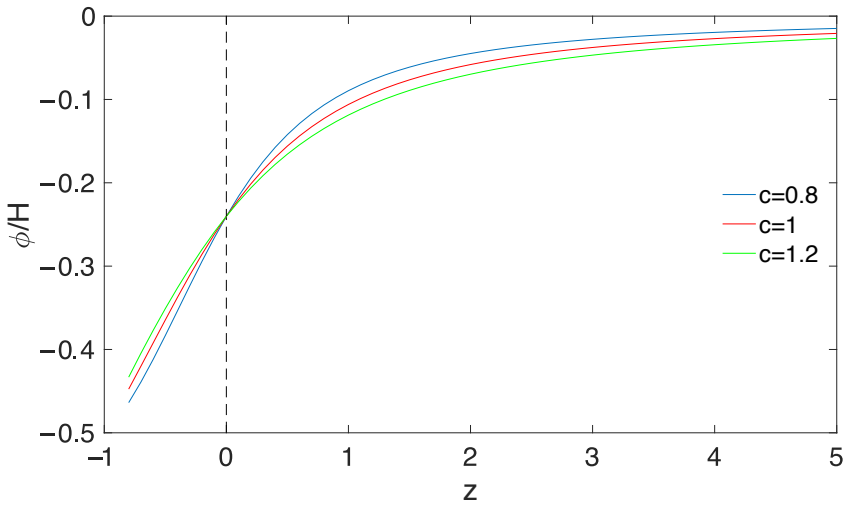

Figure 1. The evolution of the dimensionless ratio ϕ/H versus redshift z.

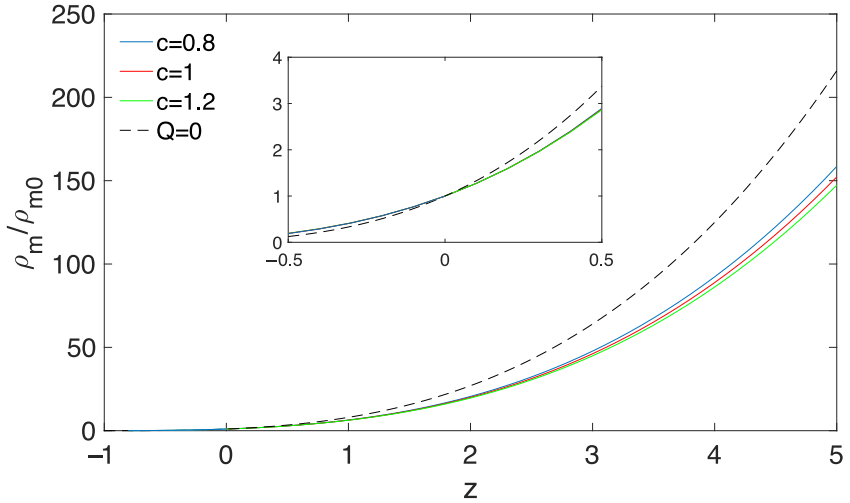

Figure 2. The evolution of the dimensionless ratio ρ_m/ρ_{m0} versus redshift z. The dashed line denotes the absence of Q, i.e., $\rho_m/\rho_{m0} = (1+z)^3$.

Additionally, according to Equations (21) and (28), from the expression (27), we obtain

$$\frac{\dot{\phi}}{H^2} = \frac{\phi\prime}{H} = \frac{1}{4}\left[(1-\sqrt{1-\Omega_{HDE}})(3-\Omega_I) + \Omega_{HDE}\left(\frac{\Omega_I}{\sqrt{1-\Omega_{HDE}}} - 1 - 2\sqrt{\frac{\Omega_{HDE}}{c^2}}\right)\right], \tag{29}$$

where the prime denotes the derivative with respect to $\ln a$. Figure 3 depicts the dimensionless ratio $\phi\prime/H$ as a function of ϕ/H. The behavior of the torsion field can be either quintessence-like ($w_\phi > -1$) or phantom-like ($w_\phi < -1$), depending on the positivity of the function $\phi'/H - 2(\phi/H)^2 - \phi/H$. From Figure 3, we see that the evolution of ϕ'/H is from decreasing to increasing with decrease in ϕ/H. We also find that, for the case of $c < 1$, the torsion field evolves from the quintessence regime to the phantom regime, which can cross the phantom line $w_\phi = -1$ and thus the torsion field is quintom-like. However, the cases of $c \geq 1$ correspond to the torsion field always lying in the quintessence regime. In particular, the case of $c = 1$ indicates that the torsion field finally tends to the cosmological constant ($w_\phi = -1$).

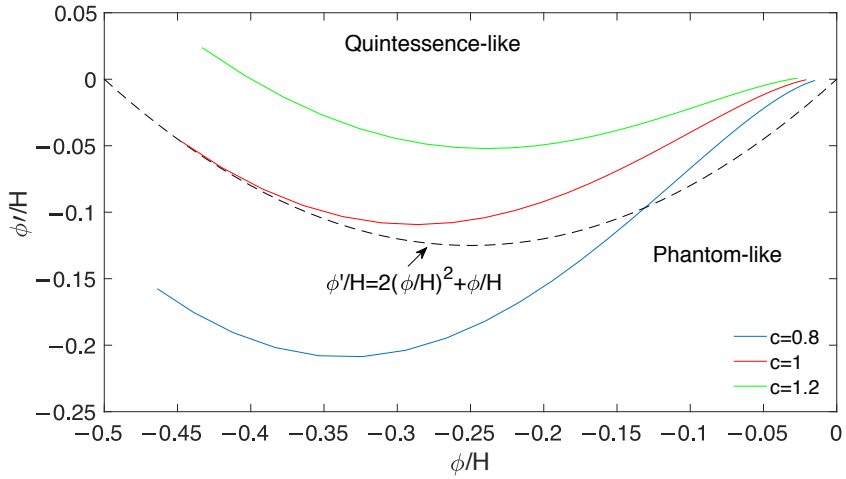

Figure 3. The dimensionless ratio $\phi\prime/H$ as a function of ϕ/H.

The same profile is exhibited by the dynamics of the effective torsion EoS w_ϕ. Substituting Equations (27) and (29) into Equation (14), we find

$$w_\phi = -\frac{2}{3}\left(\frac{\Omega_I - 3}{2\Omega_{HDE}} + \frac{1}{2} + \sqrt{\frac{\Omega_{HDE}}{c^2}}\right) - \frac{1}{\Omega_{HDE}}. \tag{30}$$

The behavior of the effective torsion EoS $w_\phi(z)$ in Figure 4 indicates that the torsion field lies in the quintessence regime during the evolution of the universe for $c \geq 1$, without crossing behavior, while the field lies in the phantom regime at present for $c < 1$. This means that the universe for the case of $c < 1$ evolves from a quintessence-like phase into a phantom-like phase with smooth crossing behavior, similar to a quintom dark energy. It is interesting to notice that the universe corresponding to $c = 1$ would asymptotically approach a de Sitter phase with $w = -1$ in the far future, which indicates that a final de Sitter stage might be a stable solution. We also note that, for all the three cases of c, the evolution curve with a rapidly increased slope exists in the interval $0 < z < 1$, which seems too fast to be consistent with observations. On the other hand, we analyze the behavior of crossing from thermodynamical consideration. At the phase transition point from quintessence to phantom, $\dot{H} = 0$ in the de Sitter spacetime case indicates that the time derivative of the temperature is $\dot{T}_h = 0$ for the reconstructed torsion model in the de Sitter stage, from the definition of Hawking temperature on the event horizon $T_h = H^2 R_h/2\pi$ [35].

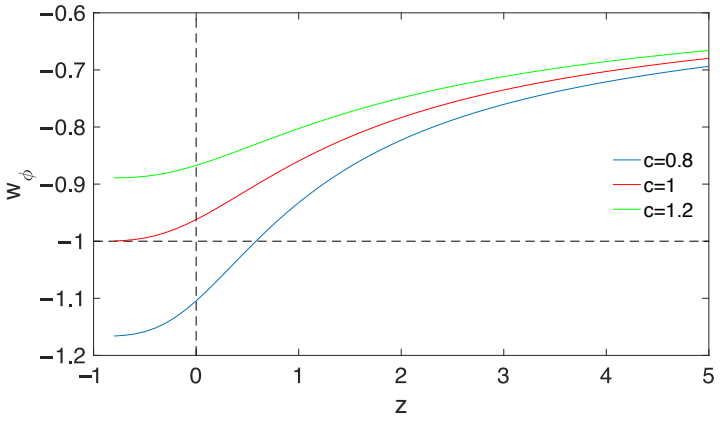

Figure 4. The evolution of the effective torsion EoS w_ϕ versus redshift z.

In order to understand the classical stability of the torsion model reconstructed from the interacting HDE, we now focus on the squared sound speed parameter, which is given by

$$v_s^2 = \frac{\dot{p}_\phi}{\dot{\rho}_\phi} = w_\phi + \dot{w}_\phi \frac{\rho_\phi}{\dot{\rho}_\phi}. \tag{31}$$

This parameter can be used to discuss how the stability of cosmological models is affected by its sign. If v_s^2 has a positive signature, the model is stable, while, for $v_s^2 < 0$, the model is unstable. Utilizing Equations (21), (28) and (30), we can obtain the expression of v_s^2 for the reconstructed torsion model. Since the analytic expression of v_s^2 is rather cumbersome to exhibit, we shall limit ourselves to plotting it as in Figure 5. It is shown that, for the cases of $c \geq 1$, $v_s^2 < 0$ for all epoch and thus the torsion model is unstable against small perturbations during the cosmic evolution. Moreover, the evolutionary trajectories of v_s^2 change slowly and almost overlap. On the other hand, for the case of $c < 1$, it is clear that $v_s^2 > 0$ transiently occurs at $-0.039 \lesssim z \lesssim 0.034$, which shows that the model is classically stable at the current epoch. This means that the case of $c < 1$ provides a more reasonable scenario to trace the cosmological evolution in the reconstructed torsion model.

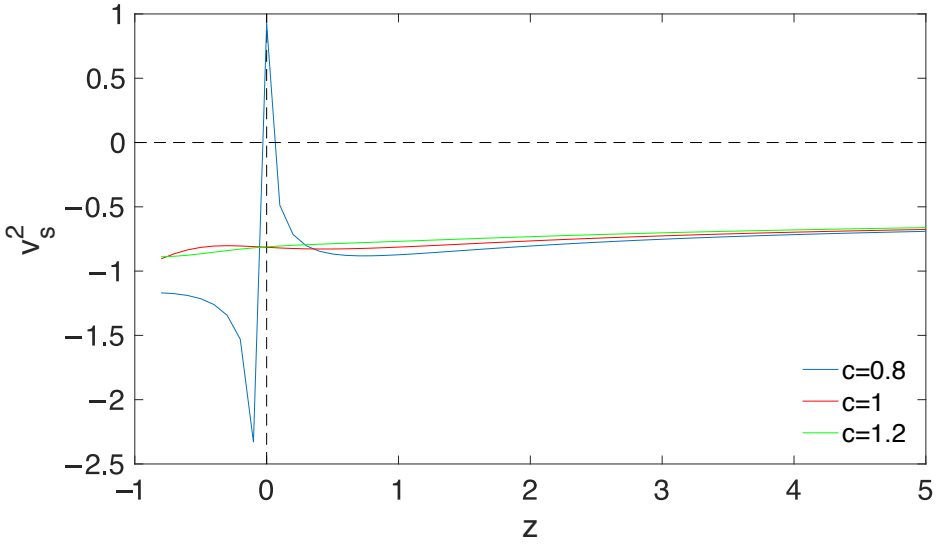

Figure 5. Square speed sound parameter v_s^2 versus redshift z.

Obviously, the accelerating mechanism of the torsion model reconstructed from the interacting HDE is bound to exhibit an essential distinction in contrast with various cosmological models. Therefore, the statefinder diagnostic for the torsion model in our scenario is sure to reveal differential features. The dimensionless statefinder pair, $\{r \equiv \dddot{a}/(aH^3), s \equiv (r-1)/3(q-1/2)\}$, introduced by Sahni et al. [36], is a natural next step beyond the Hubble parameter H and the deceleration parameter q, which cannot distinguish various accelerating mechanisms uniquely, for the reason that some models may just correspond to the same current values. It has been shown in the literature studies [37–40] that a series of cosmological models exhibit qualitatively different evolutionary trajectories in the $r-s$ plane and thus the statefinder diagnostic is a good tool to differentiate cosmological models. It is well known that the statefinder parameters for the spatially flat ΛCDM model correspond to a fixed point $\{r, s\} = \{1, 0\}$. We can clearly identify the "distance" from a given cosmological model to the ΛCDM model in the $r-s$ plane. Furthermore, the statefinder parameters can be expressed in terms of the deceleration parameter q as

$$r = 2q^2 + q - \frac{\dot{q}}{H}, \qquad s = \frac{r - 1}{3(q - \frac{1}{2})}. \tag{32}$$

According to Equations (21), (22) and (28), we can obtain the concrete expressions of the statefinder parameters for the reconstructed torsion model. Figure 6 depicts the graph of the statefinder parameters in $r-s$ plane. The arrows indicate the evolutionary directions of the model. We also compare the model with the quintessence, phantom models and ΛCDM model. We see that the case of $c<1$ behaves like quintessence model ($r>1, s<0$) at early times, then makes transition from quintessence to ΛCDM fixed point and finally gets into the phantom region ($r<1, s>0$), while, for the cases of $c \geq 1$, the evolution trajectories lie in the quintessence region throughout the expansion of the universe and the crossing of the fixed point is impossible for these two cases. It is worth noting that the trajectory for the case of $c=1$ reaches the ΛCDM fixed point in the far future. Clearly, the distance from the torsion model to the ΛCDM can be easily identified in this diagram. We also list the current values of statefinder parameters in Table 1. Thus, the model for different values of c can be distinguished from each other and from ΛCDM, quintessence, phantom models by using the statefinder diagnostic method. These results are also confirmed via the $r(q)$ analysis given in Figure 7. In the figure, a crossing of phantom line is also represented by a crossing of the dark solid line (ΛCDM). Therefore, we find that, for the case of $c<1$, the trajectory similar to the quintom dark energy model crosses the ΛCDM line. While the cases of $c \geq 1$ correspond to a quintessence-like dark energy model ($r<1$) and the universe approaches an exact de Sitter expansion for the case of $c=1$. Additionally, Figure 7 indicates that the universe has a phase transition from deceleration to acceleration, consistently with cosmological observations, independent of c. Moreover, the deceleration parameter q seems to converge to around 0.5 at the higher z, which characterize a matter dominated universe, as expected from the standard model. We can also estimate the current values of q as listed in Table 1. It is shown that q_0 is different for the three cases of c and decreases with a decreasing parameter c. Clearly, the current value q_0 is compatible with the observational result $q_0 = -0.64 \pm 0.22$ found in [41] from Union2 SNIa data.

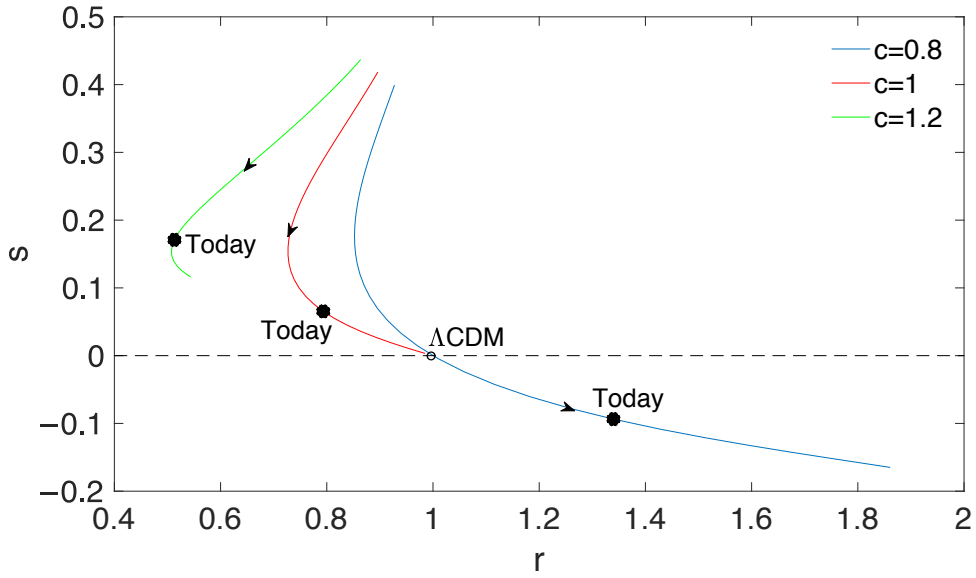

Figure 6. Evolving trajectories of the statefinder in the $r-s$ plane. The arrows denote the evolution directions of $s(r)$. The stars on the curves indicate current states of the model, and the dot symbol is related to the location of the standard ΛCDM model in the $r-s$ plane.

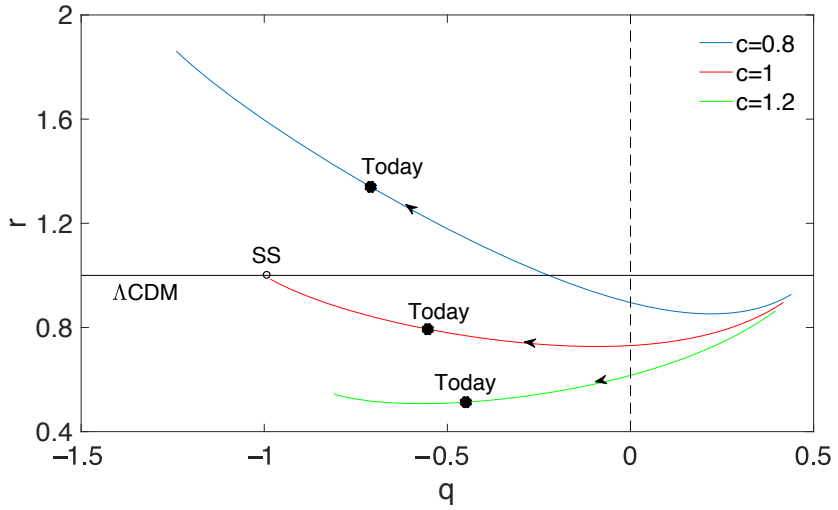

Figure 7. The parameter $r(q)$ as a function of the deceleration parameter q. The arrows denote the evolution directions of $r(q)$ and the dark line shows the time evolution of the ΛCDM model. The stars on the curves indicate current states of the model for different values of c, and the point of $(-1, 1)$ corresponds to the steady state model (SS)—the de Sitter expansion.

Table 1. Values of statefinder paramters at $z = 0$ for the three cases of the parameter c.

Statefinder Parameters	c = 0.8	c = 1	c = 1.2
r	1.3398	0.7934	0.5131
s	−0.0936	0.0654	0.1709
q	−0.7095	−0.5536	−0.4496

4. Constraints from Observational Data

The above analysis preliminarily displays that the reconstructed torsion model could be consistent with the cosmological observations. However, it is important to quantitatively judge how well the torsion model can fit with the observational data. Thus, we would like to investigate the observational constraints on the model parameters, i.e., the parameter c and the present fractional energy density of all forms of matter Ω_{m0}. In practice, the adopted samples consist of the Pantheon sample of Type Ia supernova (SNe Ia) including 1048 SNe Ia with $0.01 < z < 2.3$ [42] and the Pantheon+ sample including 1701 light curves of 1550 distinct SNe Ia with $0.001 < z < 2.26$ [43].

The likelihood is assumed to be Gaussian and thus we have the total likelihood function

$$\mathcal{L} \propto e^{-\chi^2/2}, \tag{33}$$

where χ^2 is constructed as

$$\chi^2 = \chi^2_{SNe}. \tag{34}$$

We employ an affine-invariant Markov chain Monte Carlo (MCMC) ensemble sampler (emcee) [44] to generate the posterior probability distributions for the parameters.

The two-dimensional (2D) posterior distributions of the parameters (Ω_{m0}, c) are displayed in Figures 8 and 9, corresponding to the constraints from the Pantheon and Pantheon+ samples, respectively. The mean values with 68% confidence limits for the parameters are $\Omega_{m0} = 0.305^{+0.062}_{-0.075}$ and $c = 0.979^{+0.432}_{-0.293}$ from the Pantheon sample and $\Omega_{m0} = 0.299^{+0.063}_{-0.068}$ and $c = 1.412^{+0.614}_{-0.521}$ from the Pantheon+ sample. One can see that the limits on Ω_{m0} are compatible with that of the ΛCDM model obtained from the latest Planck mission observations at 68% confidence level [45]. In addition, the mean value of

c from the Pantheon sample corresponds to the quintom-like scenario (i.e., $c < 1$) and its mean value from the Pantheon+ sample corresponds to the quintessence-like scenario (i.e., $c \geq 1$). However, both of the Pantheon and Pantheon+ samples cannot distinguish the quintom-like and quintessence-like scenarios at 68% confidence level.

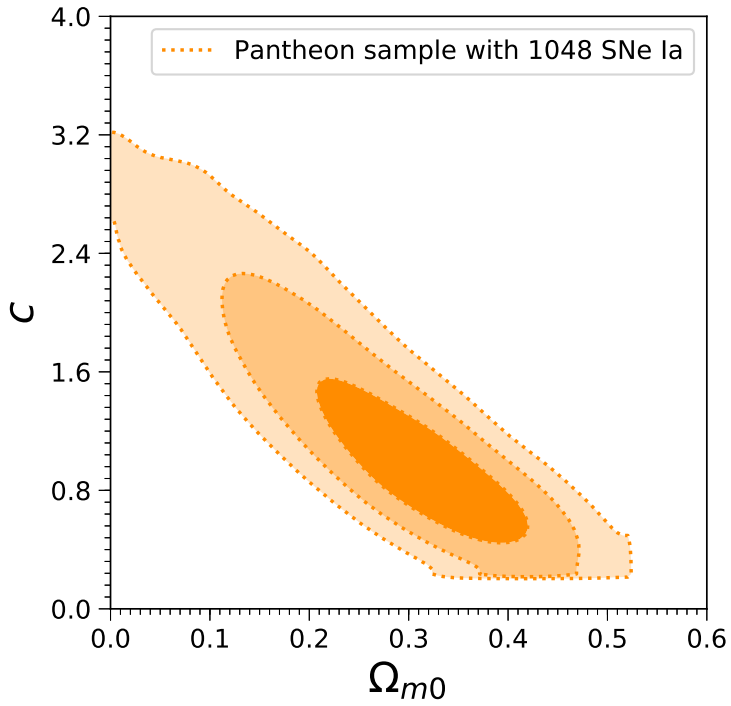

Figure 8. Confidence intervals at 68% ,95% and 99% in the (Ω_{m0}, c) plane constrained from the Pantheon SNe Ia sample including 1048 SNe Ia with $0.01 < z < 2.3$.

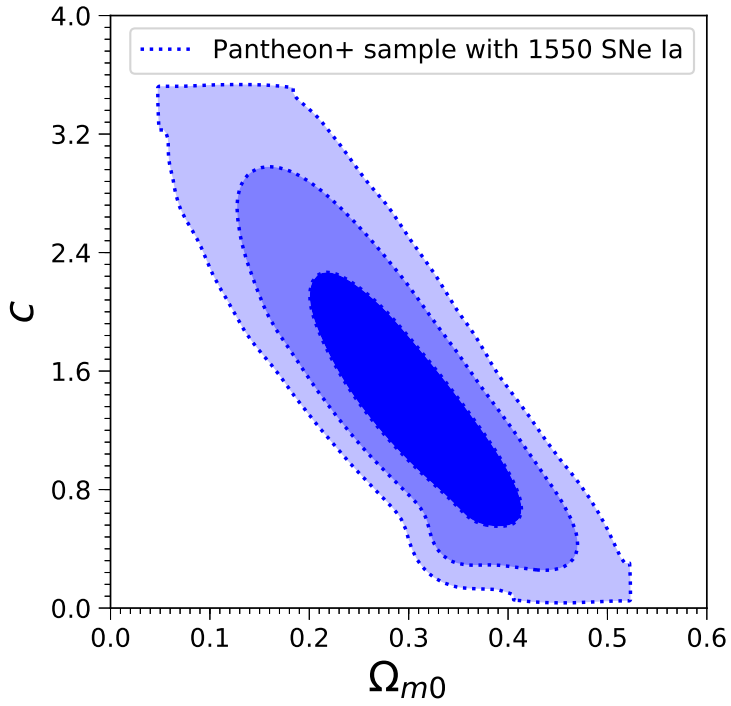

Figure 9. Confidence intervals at 68% ,95% and 99% in the (Ω_{m0}, c) plane constrained from the Pantheon+ SNe Ia sample including 1701 light curves of 1550 distinct SNe Ia with $0.001 < z < 2.26$.

5. Conclusions

In this paper, a Friedmann cosmological model in the Einstein–Cartan framework with torsion is studied. The spatially homogeneous and isotropic FLRW universe can only accommodate specific forms of torsion and therefore we consider a single scalar function of time $\phi = \phi(t)$, which is generally compatible with the FLRW symmetries, as mentioned in [26]. We reconstruct a torsion model corresponding to the holographic dark energy (HDE) density. By studying the corresponding relation between the effective energy density of torsion field ρ_ϕ and holographic dark energy density ρ_{HDE}, we naturally get a kind of torsion field from the interacting holographic dark energy with interaction term $Q = -2\phi\rho_m$.

The evolution of the dimensionless ratio ϕ/H versus redshift z indicates that it is negative during the overall evolution of the universe. Moreover, the ratio ϕ/H decreasing monotonically from zero at early times to $-1/2$ in the far future, indicates an evolution towards a completely dark energy dominated epoch. The behavior of the dimensionless ratio ρ_m/ρ_{m0} in terms of redshift shows that the model predicts the sequence of an early matter dominated era with a decelerated expansion and a late-time torsion field dominated era with an accelerated phase, for all the three cases of c. On the other hand, the behavior of the dimensionless ratio ρ_m/ρ_{m0} describes the effect of interaction Q on the energy density of matter. We find that the evolutionary trajectories of ρ_m/ρ_{m0} gradually close to the one of the non-interacting model, converge to it at the present time and then slightly deviate from it at the late time, independent of c.

The graph of the dimensionless ratio $\phi\prime/H$ as a function of ϕ/H shows that the evolution of ϕ'/H is from decreasing to increasing with decrease in ϕ/H. We find that, for the case of $c < 1$, the torsion field corresponds to a quintom-like dark energy. However, the cases of $c \geq 1$ correspond to the torsion field always lying in the quintessence regime. In particular, the case of $c = 1$ indicates that the torsion field finally tends to the cosmological constant. From the dynamics of the effective torsion EoS, we understand that, different from the case of $c \geq 1$ corresponding to the quintessence-like dark energy, the universe for the case of $c < 1$ evolves from a quintessence-like phase into a phantom-like phase with smooth crossing behavior, similar to quintom dark energy and it mimics phantom-like dark energy at present.

Additionally, the model is unstable against small perturbations during the cosmic evolution for $c \geq 1$. However, the model is classically stable at the current epoch for $c < 1$, which means that the case of $c < 1$ provides a more reasonable scenario to trace the cosmological evolution in the model.

We also compare the model with ΛCDM, quintessence and phantom models by using the statefinder diagnostic method. As a result, the model for different values of c can be distinguished from each other and from ΛCDM, quintessence, phantom models. These results are also confirmed by the $r(q)$ analysis. Additionally, the trajectory in $q - r$ plane indicates that the universe has a phase transition from deceleration to acceleration, consistently with cosmological observations, independent of c. However, the current value q_0 is different for the three cases of c and decreases with a decreasing parameter c. Moreover, q_0 is compatible with the observational result.

Finally, we constrain the model with the updated cosmological data from SNe Ia. As a consequence, the limits on the energy density parameter of matter Ω_{m0} are completely compatible with that of ΛCDM model obtained from the latest Planck mission observations at 68% confidence level. In addition, the mean value of c from the Pantheon sample corresponds to the quintom-like scenario and its mean value from the Pantheon+ sample corresponds to the quintessence-like scenario . However, both the Pantheon and Pantheon+ samples cannot distinguish the quintom-like and quintessence-like scenarios at 68% confidence level.

Author Contributions: These authors contributed equally to this work. All authors have read and agreed to the published version of the manuscript.

Funding: This research was funded by the National Key Research and Development Program of China (No. 2022YFA1602903), the National Natural Science Foundation of China (Nos. 11988101 and 12033008), the K. C. Wong Education Foundation and the Science and Technology Program Foundation of the Beijing Municipal Commission of Education of China (grant No. KM201410028003).

Data Availability Statement: Not applicable.

Conflicts of Interest: The authors declare no conflict of interest.

References

1. Riess, A.G.; Filippenko, A.V.; Challis, P.; Clocchiatti, A.; Diercks, A.; Garnavich, P.M.; Gilliland, R.L.; Hogan, C.J.; Jha, S.; Kirshner, R.P .; et al. Observational Evidence from Supernovae for an Accelerating Universe and a Cosmological Constant. *Astron. J.* **1998**, *116*, 1009–1038. [CrossRef]
2. Perlmutter, S.; Aldering, G.; Goldhaber, G.; Knop, R.A.; Nugent, P.; Castro, P.G. Measurements of Omega and Lambda from 42 High-Redshift Supernovae. *Astrophys. J.* **1999**, *517*, 565. [CrossRef]
3. Peebles, P.J.E. Improving Physical Cosmology: An Empiricist's Assessment: Prepared for a lecture at the 2021 Canadian Association of Physicists Congress. *arXiv* **2021** , arXiv:2106.02672.
4. Di Valentino, E.; Melchiorri, A.; Silk, J. Planck evidence for a closed Universe and a possible crisis for cosmology. *Nat. Astron.* **2019**, *4*, 196–203. [CrossRef]
5. Martinelli, M.; Tutusaus, I. CMB tensions with low-redshift H_0 and S_8 measurements: Impact of a redshift-dependent type-Ia supernovae intrinsic luminosity. *Symmetry* **2019**, *11*, 986. [CrossRef]
6. Di Valentino, E.; Mena, O.; Pan, S.; Visinelli, L.; Yang, W.; Melchiorri, A.; Silk, J. In the Realm of the Hubble tension-a Review of Solutions. *Class. Quantum Grav.* **2021**, *38*, 153001. [CrossRef]
7. Carroll, S.M.; Duvvuri, V.; Trodden, M.; Turner, M.S. Is cosmic speed-up due to new gravitational physics? *Phys. Rev. D* **2004**, *70*, 043528. [CrossRef]
8. Linder, E.V. Einstein's other gravity and the acceleration of the Universe. *Phys. Rev. D* **2010**, *81*, 127301. [CrossRef]
9. Kazempour, S.; Akbarieh, A.R. Cosmology in Brans-Dicke-de Rham-Gabadadze-Tolley massive gravity. *Phys. Rev. D* **2022**, *105*, 123515. [CrossRef]
10. Trautman, A. On the structure of the Einstein–Cartan equations, in Differential Geometry. *Symp. Math.* **1973**, *12*, 139.
11. Hehl, F.W.; Von Der Heyde, P.; Kerlick, G.D.; Nester, J.M. General relativity with spin and torsion: Foundations and prospects. *Rev. Mod. Phys.* **1976**, *48*, 393–416. [CrossRef]
12. Obukhov, Y.N.; Korotky, V.A. The Weyssenhoff fluid in Einstein–Cartan theory. *Class. Quantum Grav.* **1987**, *4*, 1633–1657. [CrossRef]
13. Gonzalez, P.A.; Reyes, S.; Vasquez, Y. Teleparallel equivalent of Lovelock gravity, generalizations and cosmological applications. *JCAP* **2019**, *7*, 40. [CrossRef]
14. Formiga, J.B. Conformal teleparallel theories and Weyl geometry. *Phys. Rev. D* **2019**, *99*, 064047. [CrossRef]
15. Ciufolini, I.; Matzner, R.; Paolozzi, A.; Pavlis, E.C.; Sindoni, G.; Ries, J.; Gurzadyan, V.; Koenig, R. Satellite Laser-Ranging as a Probe of Fundamental Physics. *Nat. Sci. Rep.* **2019**, *9*, 15881. [CrossRef] [PubMed]
16. Touboul, P.; Metris, G.; Rodrigues, M.; Berge, J.; Robert, A.; Baghi, Q.; Andre, Y.; Bedouet, J.; Boulanger, D.; Bremer, S.; et al. Result of the MICROSCOPE Weak Equivalence Principle test. *Class. Quantum Grav.* **2022**, *39*, 204009. [CrossRef]
17. Kostelecky, V.A.; Russell, N.; Tasson, J.D. Constraints on Torsion from Bounds on Lorentz Violation. *Phys. Rev. Lett.* **2008**, *100*, 111102. [CrossRef]
18. Ivanov, A.N.; Wellenzohn, M. Einstein–Cartan Gravity with Torsion Field Serving as Origin for Cosmological Constant or Dark Energy Density. *Astrophys. J.* **2016**, *829*, 47. [CrossRef]
19. Cruz, M.; Izaurieta, F.; Lepe, S. Non-zero torsion and late cosmology. *Eur. Phys. J. C* **2020**, *80*, 559. [CrossRef]
20. Iosifidis, D.; Ravera, L. The cosmology of quadratic torsionful gravity. *Eur. Phys. J. C* **2021**, *81*, 736. [CrossRef]
21. Poplawski, N.J. Cosmology with torsion: An alternative to cosmic inflation. *Phys. Lett. B* **2010**, *694*, 181; Erratum in *Phys. Lett. B* **2011**, *701*, 672. [CrossRef]
22. Guimarães, T.M.; Lima, R.D.C.; Pereira, S.H. Cosmological inflation driven by a scalar torsion function. *Eur. Phys. J. C* **2021**, *81*, 271.
23. Tilquin, A.; Schücker, T. Torsion, an alternative to dark matter? *Gen. Relativ. Gravit.* **2011**, *43*, 2965. [CrossRef]
24. Pereira, S.H.; Vicente, A.M.; Jesus, J.F.; Holanda, R.F.L. Dark matter from torsion in Friedmann cosmology. *Eur. Phys. J. C* **2022**, *82*, 356. [CrossRef]
25. Tsamparlis, M. Methods for deriving solutions in generalized theories of gravitation: The Einstein–Cartan theory. *Phys. Rev. D* **1981**, *24*, 1451. [CrossRef]
26. Kranas, D.; Tsagas, C.G.; Barrow, J.D.; Iosifidis, D. Friedmann-like universes with torsion. *Eur. Phys. J. C* **2019**, *79*, 341. [CrossRef]

27. Cohen, A.G.; Kaplan, D.B.; Nelson, A.E. Effective Field Theory, Black Holes and the Cosmological Constant. *Phys. Rev. Lett.* **1999**, *82*, 4971. [CrossRef]
28. Li, M. A Model of Holographic Dark Energy. *Phys. Lett. B* **2004**, *603*, 1. [CrossRef]
29. Li, M.; Li, X.D.; Wang, S.; Zhang, X. Holographic dark energy models: A comparison from the latest observational data. *JCAP* **2009**, *2009*, 36. [CrossRef]
30. Zhang, Z.; Li, S.; Li, X.D.; Zhang, X.; Li, M. Revisit of the Interaction between Holographic Dark Energy and Dark Matter. *JCAP* **2012**, *6*, 9. [CrossRef]
31. Watanabe, T.; Hayashi, M.J. General Relativity with Torsion. TOKAI-HEP/TH-2004-09. *arXiv* **2004**, arXiv:gr-qc/0409029.
32. Daouda, M.H.; Rodrigues, M.E.; Houndjo, M.J.S. Reconstruction of $f(T)$ gravity according to holographic dark energy. *Eur. Phys. J. C* **2012**, *72*, 1893.
33. Karami, K.; Asadzadeh,S.; Abdolmaleki, A.; Safari, Z. Holographic $f(T)$-gravity model with power-law entropy correction. *Phys. Rev. D* **2013**, *88*, 084034. [CrossRef]
34. Saha, P.; Debnath, U. Reconstructions of $f(T)$ Gravity from Entropy Corrected Holographic and New Agegraphic Dark Energy Models in Power-law and Logarithmic Versions. *Eur. Phys. J. C* **2016**, *76*, 491. [CrossRef]
35. Saha, S.; Chakraborty, S. A redefinition of Hawking temperature on the event horizon: Thermodynamical equilibrium. *Phys. Lett. B* **2012**, *717*, 319–322. [CrossRef]
36. Sahni, V.; Saini, T.D.; Starobinsky, A.; Alam, U. Statefinder–a new geometrical diagnostic of dark energy. *JETP Lett.* **2003**, *77*, 201–206. [CrossRef]
37. Yi, Z.L.; Zhang, T.J. Statefinder diagnostic for the modified polytropic Cardassian universe. *Phys. Rev. D* **2007**, *75*, 083515. [CrossRef]
38. Setare, M.R.; Zhang, J.; Zhang, X. Statefinder diagnosis in a non-flat universe and the holographic model of dark energy. *JCAP* **2007**, *703*, 7. [CrossRef]
39. Cao, S.L.; Li, S.; Yu, H.R.; Zhang, T.J. Statefinder diagnostic and constraints on the Palatini $f(R)$ gravity theories. *Res. Astron. Astrophys.* **2018**, *18*, 26. [CrossRef]
40. Barrow, J.D.; Tsagas, C.G.; Fanaras, G. Friedmann-like universes with weak torsion: A dynamical system approach. *Eur. Phys. J. C* **2019**, *79*, 764. [CrossRef]
41. Li, Z.; Wu, P.; Yu, H. Examining the cosmic acceleration with the latest Union2 supernova data. *Phys. Lett. B* **2011**, *695*, 1. [CrossRef]
42. Scolnic, D.M.; Jones, D.O.; Rest, A.; Pan, Y.C.; Chornock, R.; Foley, R.J.; Smith, K.W. The Complete Light-curve Sample of Spectroscopically Confirmed Type Ia Supernovae from Pan-STARRS1 and Cosmological Constraints from The Combined Pantheon Sample. *Astrophys. J.* **2018**, *859*, 101. [CrossRef]
43. Brout, D.; Scolnic, D.; Popovic, B.; Riess, A.G.; Carr, A.; Zuntz, J.; Kessler, R.; Davis, T.M.; Hinton, S.; Jones, D.; et al. The Pantheon+ Analysis: Cosmological Constraints. *Astrophys. J.* **2022**, *938*, 110. [CrossRef]
44. Foreman -Mackey, D.; Hogg, D.W.; Lang, D.; Goodman, J. emcee: The MCMC Hammer. *Publ. Astron. Soc. Pac.* **2013**, *125*, 306. [CrossRef]
45. Aghanim, N.; Akrami, Y.; Ashdown, M.; Aumont, J.; Baccigalupi, C.; Ballardini, M.; Roudier, G. Planck 2018 results. VI. Cosmological parameters. *A&A* **2020**, *641*, A6.